16th World Conference on Earthquake, 16WCEE 2017

Santiago Chile, January 9th to 13th 2017

Paper N° 4221 (Abstract ID)

Registration Code: S-S1464075038

APPLICATION OF NEW STRESS TEST CONCEPTS TO CRITICAL INFRASTRUCTURES. THE CASE OF THESSALONIKI PORT IN GREECE

K. Pitilakis[(1)], S. Fotopoulou[(2)], S. Argyroudis [(3)], S. Karafagka [(4)], K. Kakderi [(5)], J. Selva [(6)]

[(1)] *Professor, Aristotle University, Thessaloniki, Greece, kpitilak@civil.auth.gr*
[(2)] *Researcher, Aristotle University, Thessaloniki, Greece, sfotopou@civil.auth.gr*
[(3)] *Researcher, Aristotle University, Thessaloniki, Greece, sarg@civil.auth.gr*
[(4)] *PhD student, Aristotle University, Thessaloniki, Greece, stellak@civil.auth.gr*
[(5)] *Researcher, Aristotle University, Thessaloniki, Greece, kkakderi@civil.auth.gr*
[(6)] *Researcher, Istituto Nazionale di Geofisica e Vulcanologia, Bologna, Italy, jacopo.selva@ingv.it*

Abstract

A new engineering risk based methodology for stress tests named ST@STREST developed in the context of the European project STREST (www.strest-eu.org) for non-nuclear critical infrastructures (CIs) is applied to the port of Thessaloniki in North Greece. This case study is a characteristic example of distributed and/or geographically extended infrastructures with potentially high economic and environmental impact, which is exposed to seismic, geotechnical (i.e. liquefaction) and tsunami hazards. The ST@STREST workflow consists of four phases: Pre-Assessment, Assessment, Decision and Report phase, which are performed in sequence. In the pre-assessment phase, all the necessary information of the port is collected and archived in a GIS database. The inventory includes buildings, waterfronts, cranes and their interdependencies with the electric power supply system. Geotechnical, geophysical and topobathymetric data were also collected in this phase. Fragility models for all exposed elements and considered hazards are either selected from the literature or developed as case specific models. Risk measures and objectives are defined related to the functionality of the system and the structural losses. The assessment phase includes the component and the system level assessments. In the first level, the performance of each component is evaluated using a risk-based approach for seismic and tsunami hazards to check whether the component passes or fails the minimum requirements for its performance implied by the code, stakeholders and decision-makers needs. Then, a system level probabilistic risk analysis (PRA) is conducted separately for earthquake and tsunami hazards considering epistemic uncertainties. To reduce the uncertainties in site specific response, a scenario-based risk analysis (SBRA) is also carried out focusing on extreme seismic events. In the Decision phase, the results of risk assessments are compared with the objectives defined in Pre-Assessment phase in order to assess the performance of the CI and decide whether it passes, partly passes or fails the test. This phase also includes identification of critical events and components and strategies to improve the performance and resilience of the port system. In the ultimate phase the results are presented to the port Authority and regulators.

Keywords: Stress test; probabilistic risk assessment; scenario-based risk assessment; systemic analysis; Thessaloniki port

1. Introduction

A safer and more resilient society requires improved and standardized tools for hazard and risk assessment of low-probability high-consequences (LP-HC) events (so-called extreme events) and the systematic application of these new tools to whole classes of critical infrastructures (CIs). The European research project STREST: "Harmonized approach to stress tests for critical infrastructures against natural hazards" (www.strest-eu.org), proposed a new engineering risk based multi-level framework for stress tests named ST@STREST for non-nuclear CIs of different classes [1]. The methodology is based on a common CI taxonomy and rigorous models for the hazard, vulnerability, performance and resilience assessment under different natural hazards. Different levels of stress tests are proposed, based on the complexity of the analysis (e.g. quantification of epistemic uncertainty, expert elicitation) and the risk assessment approaches (single or multi-hazard, probabilistic or scenario based). The port of Thessaloniki, one of the most important ports in Southeast Europe and the largest transit-trade port in Greece, is one of the case studies, a characteristic example of distributed and/or geographically extended infrastructures with potentially high economic and environmental impact. The port occupies a total space of 1.5 million m^2, includes 6 piers spreading on a 6200 m long quay and a sea depth down to 12 m, with open and indoors storage areas, suitable for servicing all types of cargo and passenger traffic. The port also has installations for liquid fuel storage, while is located in proximity to the international natural-gas pipeline and is linked to the national and international road and railway network (www.thpa.gr).

The goal of this study is to apply the ST@STREST framework to the port infrastructures exposed to different seismic hazards i.e. ground shaking, liquefaction and tsunami. The framework consists of four phases: Pre-Assessment, Assessment, Decision and Report phase as described in Fig. 1. In the pre-assessment phase all the necessary data is collected and archived in a GIS database. The inventory includes port facilities, various buildings, quay walls, cranes and networks (e.g. electric power supply system). The vulnerability of the infrastructures to the given hazards is assessed using site and case specific or generic fragility functions. Specific risk metrics are defined related to the functionality of the port system and the structural losses. The stress test levels are defined and set-up according to ST@STREST framework. In the first level, a risk-based assessment of each component is carried out for earthquake and tsunami hazards to check whether the component passes or fails the minimum requirements for its performance. For that, the target (acceptable) probability of collapse implied by the code, stakeholders and decision-makers needs should be pre-defined for each component. Then, a probabilistic risk analysis (PRA) is conducted for the whole system separately for earthquake and tsunami hazards considering specific interdependencies between network and components. Site specific response and extreme seismic events are evaluated with a scenario-based risk analysis (SBRA). The estimated response is compared with predefined acceptable risk criteria in order to assess the performance of the CI and decide whether it passes, partly passes or fails the test for all possible events and to define how much the safety of the CI should be improved until the next periodical verification [1]. The decision phase also includes disaggregation and sensitivity analysis for the identification of the critical components and events, guidelines and strategies to improve the performance and the resilience of the port as a critical facility.

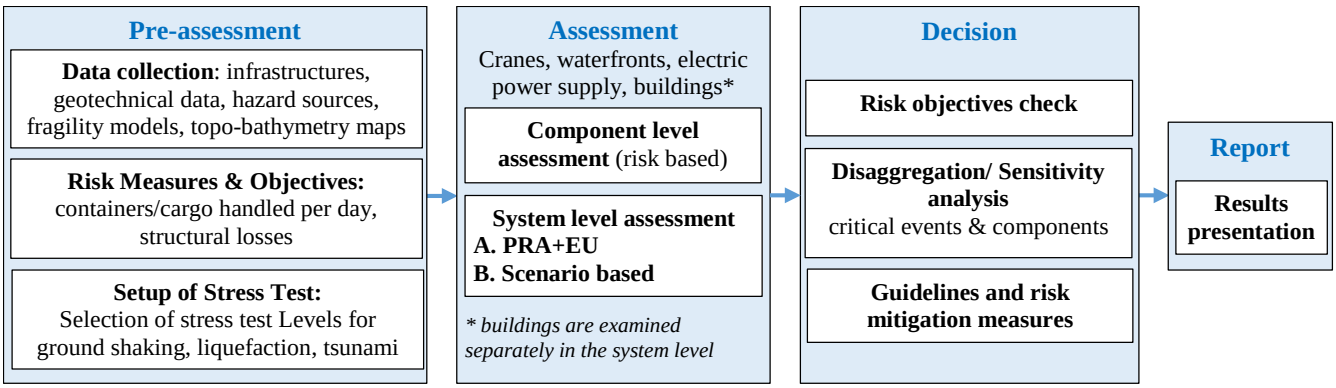

Fig. 1 – Flowchart of the ST@STREST framework for the stress test application in the port of Thessaloniki.

2. Pre-assessment phase

A GIS database for the port facilities was developed by the Research Unit of Soil Dynamics and Geotechnical Earthquake Engineering (SDGEE, sdgee.civil.auth.gr) at Aristotle University of Thessaloniki in collaboration with the Port Authority in the framework of previous national and European projects and it is further updated in STREST project (www.strest-eu.org). Waterfront structures, cargo handling equipment, buildings (offices, sheds, warehouses etc.) and the electric power supply system are examined (Fig. 2). The SYNER-G (www.syner-g.eu, [2]) taxonomy is used to describe the different typologies. Waterfront structures include concrete gravity block type quay walls with simple surface foundation and non-anchored components. Cargo handling equipment has non-anchored components without back-up power supply. Four gantry cranes are used for container loading-unloading services located in the western part of the 6th pier. The electric power supply to the cranes is assumed to be provided through non-vulnerable lines from the distribution substations that are present inside the port facilities. They are classified as low-voltage substations, with non-anchored components. In total, 85 building and storage facilities are considered in the analyses. The majority is reinforced concrete (RC) buildings comprising principally of low- and mid-rise infilled frame and dual systems with low or no seismic design. The steel buildings are basically warehouses with one or two floors while the unreinforced masonry (URM) buildings are old low-rise and mid-rise structures.

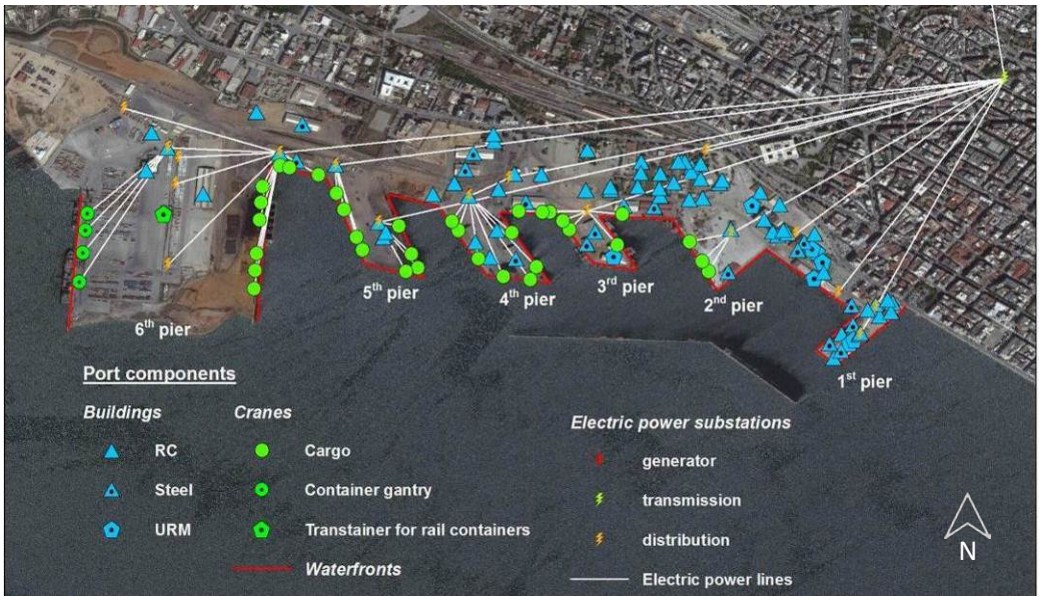

Fig. 2 – Geographical representation of Thessaloniki's port infrastructures considered in the study.

Soft alluvial deposits, sometimes susceptible to liquefaction, characterize the Port subsoil conditions. The seismic rock basement is found from 150 to 180 m, while a comprehensive set of field and laboratory tests provide all necessary information to perform any kind of site specific ground response analyses [3]. Complementary geophysical tests including array microtremor measurements have been conducted in the frame of STREST project [4]. All available data (Fig. 3) are properly archived.

The vulnerability of the Port facilities is assessed through fragility functions, which describe the probability of exceeding predefined damage states (DS) for given levels of peak ground acceleration (PGA), permanent ground displacement (PGD) and inundation depth for the ground shaking, liquefaction and tsunami hazards respectively (Table 1). The fragility functions used to assess the damages due to liquefaction are generic [5], while the models used for ground shaking and tsunami are either case specific or generic. Analytical tsunami fragility curves have been developed for representative typologies of the Port RC buildings, warehouses and gantry cranes [6]. For simplicity reasons the waterfront structures are considered as non-vulnerable to tsunami forces.

Fig. 3 – Location of geotechnical and geophysical field measurements in Thessaloniki's port area.

Table 1 – Fragility functions used in the risk analyses.

Hazard	Component	Intensity measure	Reference
Ground shaking	RC and URM buildings	PGA	[7]
	Steel buildings		[5]
	Waterfront structures		[8]
	Cranes/cargo handling equipment		
	Electric power substations (distribution, transmission)		[5, 9]
Liquefaction	Buildings/ Housed electric power substations (all considered typologies)	PGD	[5]
	Waterfront structures		
	Cranes/cargo handling equipment		
Tsunami	RC Buildings/ Electric power substations	Inundation depth	[6]
	Warehouses (Steel and URM buildings)		
	Cranes/cargo handling equipment		

In this phase, specific risk measures and objectives are also defined related to the functionality of the port system and the structural losses. Since two terminals (container, bulk cargo) are assumed, the system performance is measured through the total number of containers handled (loaded and unloaded) per day (TCoH), in Twenty-foot Equivalent Units (TEU), and the total cargo handled (loaded and unloaded) per day (TCaH), in tones. Risk measures related to structural and economic losses of the buildings are also set for the tsunami case and the scenario based assessment. The risk objectives correspond to the boundaries of the grading system proposed in ST@STREST [1]. The CI passes the stress test if is classified into grade AA (negligible risk) or A (risk being as low as reasonably practicable, ALARP). The CI partly passes the stress test if it receives grade B (possibly unjustifiable risk), while it fails the stress test if it is classified into grade C (intolerable risk). Since no regulatory boundaries exist for the moment for port facilities, continuous (i.e. straight lines on the logarithmic performance curve, see Fig. 4) and scalar (i.e. expected performance loss, see Table 2) boundaries were defined in this application based on general judgement criteria for the probabilistic and scenario based system-wide risk assessment respectively in order to demonstrate the application of the ST@STREST. Finally, the stress test levels are defined and outlined in the following section.

3. Assessment phase

3.1 Component level assessment for single hazard

The aim is to check each component of the port independently for earthquake and tsunami hazards in order to show whether the component passes or fails the pre-defined minimum performance requirements implied by the current codes. A risk-based assessment is performed using the hazard function at the location of the component and the fragility function of the component. These two functions are convolved in risk integral in order to obtain probability of exceedance of a designated limit state in a period of time (P_f). This probability is estimated on the basis of closed form risk equation [10] as follows:

$$P_f = \mathrm{H}(\overline{IM})\ \exp(0.5\ \mathrm{k}^2\beta^2) \quad (1)$$

where $\overline{IM}$ and β are the median and log-standard deviation values respectively of the fragility function, H(*IM*) is the hazard function and k is the logarithmic slope of the hazard function idealized in the following form:

$$\mathrm{H}(IM) = \mathrm{k_o}\cdot IM^{-\mathrm{k}} \quad (2)$$

where k_o is a constant that depends on the seismicity of the site. Proper k and k_o can be obtained by fitting the actual hazard curve provided that the entire hazard function or at least two points from the hazard function are available. For the seismic case, k and k_o were computed from the hazard curve corresponding to return periods equal to 475 and 4975 years for the normal and the extreme event respectively based on site specific response analyses for three representative soil profiles (Section 3.3). For the tsunami case, at least two points of the mean hazard function estimated from probabilistic tsunami hazard assessment at various locations in the port area were used to estimate these parameters (Section 3.2.2). The target (acceptable) probability of exceedance of a designated limit state for a period of time implied by the code, stakeholders and decision makers (P_t) also has to be defined for each component and different limit states. In this application the target probability of exceedance of the collapse damage state is only provided. This probability was set to 10^{-5} based on the existing practice [e.g. 11, 12] corresponding to an acceptable probability equal to 0.05% in 50 years and was properly modified based on EC8 prescriptions to account for the importance factor γ_I of the structure. To check whether or not the component is safe against collapse, the target probability (P_t) is compared with the corresponding probability of exceeding the ultimate damage state (P_f).

As an example the proposed performance assessment approach is applied here to a strategic building of the Port, the passenger terminal, which is a low-rise infilled dual system (γ_I =1.2). The probability of exceeding the ultimate damage state (P_f), which in this study corresponds to the collapse damage state, is computed and compared with the target probability of collapse (P_t) for both earthquake and tsunami hazards. The hazard function at the location of the structure is estimated as 10^{-5} and $1.7\cdot10^{-4}$ for the seismic and tsunami case respectively, while the corresponding probabilities of collapse (P_f) are finally computed equal to $1.4\cdot10^{-3}$ and $2.0\cdot10^{-4}$. These probabilities are higher than the target (acceptable) probability of collapse (P_t) estimated equal to $4.7\cdot10^{-6}$ and $7.9\cdot10^{-6}$ for the seismic and tsunami case respectively, indicating that the structure is not safe against exceedance of the collapse limit state due to the considered hazards. Similar results are generally produced for all buildings and infrastructures providing a general assessment of the performance and resilience of the Port.

3.2 Probabilistic risk assessment at system level for single hazard

The system wide probabilistic risk assessment is made separately for ground shaking, including liquefaction, and tsunami hazard, according to the methodology developed in SYNER-G [13] and extended in STREST [14]. The objective is to evaluate the probability or mean annual frequency (MAF) of events with the corresponding loss in the performance of the port operations. The analysis is based on an object-oriented paradigm where the system is described through a set of classes, characterized in terms of attributes and methods, interacting with each other. The physical model starts from a pre-defined taxonomy and requires: a) a description of the functioning of the

system (intra-dependencies) under undisturbed and disturbed conditions (i.e., in the damaged state following an event); b) a model for the physical and functional damageability of each component (fragility functions); c) identification of all dependencies between systems (inter-dependencies); and d) definition of Performance Indicators (PIs) for components and the system as a whole (risk metrics). The computational modules include the modelling of hazard events and intensity parameters (hazard class), physical damages of components and performance of the system (network class), and specific interactions among systems (interdependency models). A Monte Carlo simulation is carried out sampling events and corresponding damages for the given hazard. The exceedance probability of different levels of performance loss for the system is assessed under the effect of any possible event, and the performance curve is produced, which is equivalent of risk curves for non-systemic probabilistic assessments in single [e.g. PEER formula, 15] and/or multi-risk [e.g. 16] analysis.

In the present application the systemic analysis concerns the container and bulk cargo movements affected by the performance of the piers, berths, waterfront and container/cargo handling equipment (cranes), while the interdependency considered is the supply of Electric Power Network (EPN) to the cranes. The capacity of berths is related to the capacity of cranes (lifts per hour/tons per hour). The functionality state of each component and the whole port system is assessed based on the computed physical damages, taking also into account system inter- and intra-dependencies. We assume that if a crane node is not fed by the reference EPN node (i.e. electric supply station) with power and the crane does not have a back-up supply, then the crane itself is considered out of service. The functionality of the demand node is based on connectivity analysis [13].

3.2.1 Seismic risk assessment

The seismic hazard model provides the means for: (i) sampling events in terms of location (epicentre), magnitude and faulting type according to the seismicity of the region and (ii) maps of sampled correlated seismic intensities at the sites of the vulnerable components in the infrastructure [17]. When the fragility of components is expressed with different IMs, the model assesses them consistently. Five seismic zones with M_{min}=5.5 and M_{max}=7.5 are selected based on the results of SHARE European research project [18] (www.share-eu.org) and the ground motion prediction equation (GMPE) of Akkar and Bommer [19] to estimate the outcrop ground motion parameters. Seismic events are sampled for the seismic zones affecting the port area through a Monte Carlo simulation (10,000 runs). The spatial variability is modelled using the correlation models provided by Jayaram and Baker [20]. For each site of a regular grid of points discretizing the study area, the averages of primary IM (PGA) from the specified GMPE were calculated, and the residual was sampled from a random field of spatially correlated Gaussian variables according to the spatial correlation model. The primary IM is then retrieved at vulnerable sites by distance-based interpolation and finally the local IM is sampled conditionally on primary IM. To scale the hazard to the site condition the site amplification factors proposed in EC8 [21] are used in accordance with the site classes that were defined in the study area. HAZUS [5] and the modelling procedure by Weatherill et al. [17] are applied to estimate the (PGDs) due to liquefaction. The computed PIs are normalized to the value referring to normal (non-seismic) conditions assuming that all cranes are working at their full capacity 24 hours per day. Fig. 4 (left panel) shows the MAF of exceedance curves (“performance curve”) for TCoH and TCaH. For performance loss values below 40% TCaH yields higher values of exceedance frequency, while for performance loss over 40% TCoH yields higher values of exceedance frequency.

3.2.2 Tsunami risk assessment

A full SPTHA (Seismic Probability Tsunami Hazard Analysis) for tsunami of seismic origin, following Lorito et al. [22] has been developed and carried out, based on inundation simulation of the Thessaloniki area [23]. Different potential tsunamigenic sources should be considered, such as earthquakes, landslides, meteorite impacts or atmospheric phenomena. Here, we focus only on tsunami of seismic origin, which is in most of cases the dominant component [24]. A very large number of numerical simulations of tsunami generation, propagation and inundation on high resolution topo-bathymetric models are in principle required, in order to give a robust evaluation of SPTHA at a local site. To reduce the computational cost, while keeping results stable and consistent with respect to explore the full variability of the sources, a method has been developed to approach the uncertainty in SPTHA [23, 25, 26], based on four steps: 1) a full exploration of the aleatory uncertainty through an Event Tree (ET) [22, 25] that accounts for all available sources of information [e.g., 27]; 2) the propagation of all potential sources till off-shore [28]; 3) a 2-stage filtering procedure based on Cluster Analysis

on the results off-shore in order to define a sub-set of "representative" events which approximate the hazard in the target area, in order to enable the inundation modelling [22]; 4) the quantification of epistemic uncertainty through Ensemble modelling based on (weighted) alternative implementations of steps 1 to 3 [25, 29].

For Thessaloniki port [23, 26], at steps 1 and 2, we considered a regional SPTHA which accounts for all the potential seismic sources from the Mediterranean Sea (>107 sources), implementing a large number of alternative models to explore the epistemic uncertainty (>105). Then, the 2-layer filtering procedure has been applied, obtaining 253 representative scenarios, which may be modelled to approximate the total hazard [22, 23]. The numerical simulations were performed using a non-linear shallow-water multi-GPU code (HySEA) [30], using 4-level nested bathymetric grids with refinement ratio equal to 4 and increasing resolution from 0.4 arc-min (~740 m) to 0.1 arc-min (~185 m) to 0.025 arc-min (~46 m) to 0.00625 arc-min (~11 m). The results have been input to an Ensemble model, in order to quantify in each point of the finest grid hazard curves, along with epistemic uncertainty, for two intensity measures: maximum flow depth and maximum momentum flux.

To assess the tsunami risk a hazard module has been developed in order to enable sampling among the 253 representative scenarios, considering the probability of occurrence of the cluster of sources that each scenario represents [22]. This procedure is possible for any preselected alternative model of input to the SPTHA ensemble, enabling the propagation of hazard epistemic uncertainty into risk analysis. The inundation simulation results for each sampled scenario are then loaded, in order to retrieve the tsunami intensity for any selected location. Note that, since the SPTHA analysis is based on an explicit simulation of each scenario, spatial correlations of the tsunami intensity are automatically accounted for. Given that the inundation simulation does not integrate potential collapses, tsunami intensity should be retrieved in proximity of each component's perimeter and outside the structure. In order to avoid any unwanted biases (e.g., retrieve the tsunami intensity over the roof of buildings, where the modelled tsunami flow depth is subtracted the height of the building), a characteristic radius has been assigned to each component, and the largest intensity value within the defined circle is obtained. Damages and non-functionalities are then sampled from the respective fragility curves (Table 1) and the retrieved tsunami intensities. The analysis has been implemented for the Port infrastructures (cranes, electric power network components and individual buildings) and the PIs are evaluated. In Fig. 4 (middle panel) we show an example for one of the alternative models (i.e. the epistemic uncertainty is not considered here). The container terminal is not expected to experience any loss (TCoH), while the loss in the cargo terminal (TCaH) is very low. This is due to the non-vulnerable condition of waterfront structures, the high damage thresholds for the cranes (i.e. inundation values that are not expected in the study area) and the distance of the electric power substations from the shoreline. The annual probabilities for buildings collapses are also low (Fig. 4, right panel). As an example 10% of the total buildings in the Port (~9 structures) will be completely damaged under tsunami forces with annual probability equal to $5 \cdot 10^{-5}$.

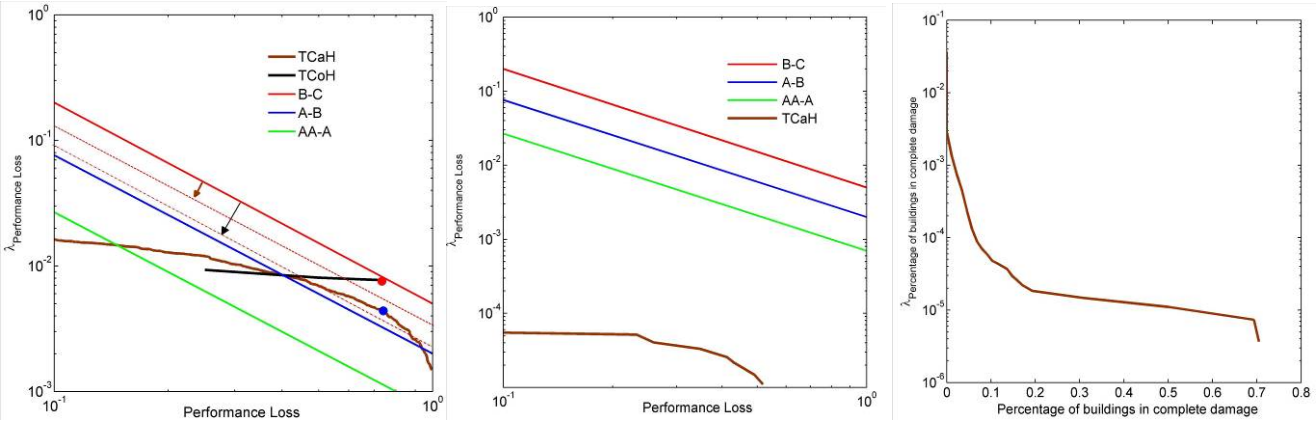

Fig. 4 – MAF of exceedance values for: the port system PIs (TCoH, TCaH) in terms of normalized performance loss (1-PI/PI_{max}) for the seismic (left) and tsunami (middle) hazard case and the buildings in collapse state for the tsunami case (right). The green, blue and red continuous lines correspond to the boundaries between risk grades AA (negligible), A (ALARP), B (possibly unjustifiable risk), and C (intolerable).

3.3 Scenario based risk assessment at system level

A scenario-based system-wide seismic risk analysis is performed complementary to the PRA approach to identify as accurately as possible the site response and to reduce the corresponding uncertainties. Two different seismic scenarios were defined in collaboration with a pool of experts: the standard seismic design scenario and an extreme scenario corresponding to return periods of T_m=475 years and T_m=4975 years respectively. To perform the site response analyses a target spectrum for seismic bedrock conditions (V_s=700-800 m/s) and a suite of acceleration time histories are needed. For the 475 years scenario, the target spectrum is defined based on the disaggregation of the probabilistic seismic hazard analysis [9, 31]. This study has provided the maximum annual exceedance probability for a certain PGA value with a moment magnitude M_w=5.7 and an epicentral distance R_{epi}=14.5 km. For the 4975 years scenario a characteristic magnitude of M_w=7.0, close to the maximum magnitude of the seismogenic source was assumed. The GMPE proposed by Akkar and Bommer [19] is applied, similarly to the probabilistic assessment. In addition to magnitude and distance, both hazard scenarios include an error term ε (which measures the number of standard deviations of logarithmic residuals σ to be accounted for in GMPE) responsible for an appreciable proportion of spectral ordinates and the contribution from ε grows with the return period. Thus, the median spectral values plus 0.5 standard deviations and 1 standard deviation are considered for the 475 years and the 4975 years scenarios respectively. A set of 15 accelerograms is selected for the 475 years scenario referring to rock or very stiff soils that on average fit the target spectrum. For the extreme scenario, 10 synthetic accelerograms are computed to fit the target spectrum (4975 years scenario I) and broadband ground motions are generated using 3D physics-based “source-to-site” numerical simulations (4975 years scenario II) [32].

Three representative soil profiles (denoted as A, B and C) are considered for the site response analyses (Fig. 2) with fundamental periods T_o equal to 1.58s, 1.60s and 1.24s respectively. The soil profiles have been defined based on previous studies and new measurements. 1D equivalent-linear (EQL) and nonlinear (NL) site response analyses including also the potential for liquefaction are carried out for the three soil profiles using as input motions at the seismic bedrock the ones estimated for the 475 and 4975 years seismic scenarios (I and II). The numerical codes Strata [33] and Cyclic1D [34] are used. To investigate the impact of the uncertainty in the shear wave velocity (V_s) profiles, the analyses are performed for the basic geotechnical models, considering a standard deviation of the natural logarithm of the Vs equal to 0.2. In particular, 100 realizations of the V_s profiles are considered in Strata using Monte Carlo simulations and the calculated response from each realization is then used to estimate statistical properties of the seismic response. In total 1500 and 1200 simulations are performed for the 475 and 4975 (I and II) scenarios respectively. The randomization of the V_s and the incorporation in Monte Carlo simulations is performed through the model proposed by Toro [35]. The corresponding site response variability was assessed in Cyclic1D considering expect for the basic Vs model, upper-range and lower-range models utilizing a logarithmic standard deviation for the V_s profile equal to 0.2 consistently with the Strata simulations. For the EQL approach the results are presented in terms of PGA(z), acceleration response spectra and spectral ratios. For the NL approach, the variation of horizontal and vertical PGD, maximum shear strain and stress, effective confinement and excess pore water pressure with depth were also computed for each analysis. Representative results for one scenario (4975 years I) for profile A are shown in Fig. 5.

The EQL approach predicts significantly larger PGA and spectral values compared to the NL approach, while its spectral shapes are flatter and have less period-to-period fluctuations than the NL one. The lower spectral values predicted by the NL approach for the extreme seismic scenario could be attributed to the liquefaction that may also result in large permanent ground deformations. The results of the NL approach indicate (although not presented herein) that liquefaction is evident for all soil profiles and scenarios. Moreover, for the extreme scenario the liquefiable layers are extended to greater depths (up to 35m, e.g. see Fig. 5 bottom-left). Among the three representative soil profiles, liquefaction effects are shown to be more pronounced in profile A.

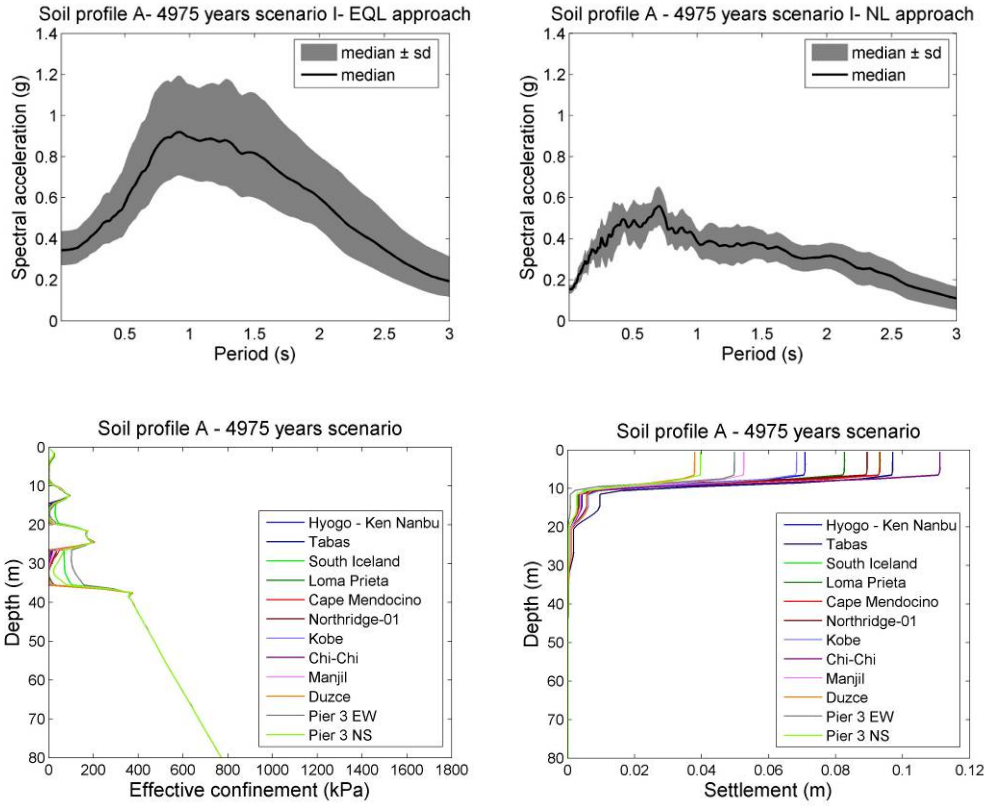

Fig. 5 – Top: Median ± standard deviation elastic 5% response spectra at the ground surface for soil profile A using the EQL (left) and NL (right) approaches. Bottom: Variation of effective confinement (left) and settlement with depth (right) for soil profile A.

The risk assessment is initially performed taking into account the potential physical damages and corresponding losses of the different components of the port. Buildings, waterfront structures, cargo handling equipment and the power supply system are examined using the fragility models for ground shaking and liquefaction (Table 1). The vulnerability assessment is performed for the 475 and 4975 years scenarios (I and II) based on the EQL and NL site-response analyses. The results from soil profile A, B or C were considered in the fragility analysis, depending on the proximity of each component to the location of the three soil profiles. In particular, for the EQL approach, the calculated PGA values at the ground surface from the total analysis cases (i.e. 2200 analyses) for each soil profile were taken into account for the vulnerability assessment due to ground shaking. For the NL approach, except for the PGA values, the PGD (horizontal and vertical) values at the ground surface were also considered to evaluate the potential damages due to liquefaction effects. Finally, the combined damages are estimated by combining the damage state probabilities due to the liquefaction (P_L) and ground shaking (P_{GS}), based on the assumption that the two damage types are independent (NIBS, 2004). Once the probabilities of exceeding the specified DS are estimated, a damage index d_m is evaluated, to quantify the structural losses as the ratio of repair to replacement cost taking values from 0: no damage (cost of repair equals 0) to 1: complete damage (cost of repair equals the cost of replacement).

The spatial distribution of the estimated losses for buildings indicates that a non-negligible percentage of the port buildings is expected to suffer significant losses (higher than moderate). This percentage ranges from 7% for the design scenario (NL approach) to 37% for the 4975 years scenario I (EQL approach). This is to be expected taking into account that all buildings were constructed with low or no seismic code provisions. Among the considered typologies, the RC structures appear to be less vulnerable compared to the steel and URM systems. The estimated losses are also significantly dependent on the analysis approach. In particular, the EQL approach is associated with higher damages and losses even for the design scenario, while for the NL approach the losses to the cranes, waterfronts and electric power substations are expected solely for the 4975 scenario I.

Table 2 – Estimated normalized performance loss of the port system for TCaH and TCoH and comparison with risk objectives for the scenario based assessment.

Scenario	Analysis type	Performance loss ($1-PI/PI_{max}$)		Risk objectives			Stress test outcome	
		TCaH	TCoH	AA-A	A-B	B-C	TCaH	TCoH
475 years	EQL	0.67	1.00	0.10	0.30	0.50	Fail	Fail
	NL	0.00	0.00				Pass	Pass
4975 years I	EQL	1.00	1.00	0.30	0.50	0.70	Fail	Fail
	NL	1.00	1.00				Fail	Fail
4975 years II	EQL	0.67	1.00				Partly pass	Fail
	NL	0.00	0.00				Pass	Pass

The systemic risk is assessed following the methodology presented in the previous section (PRA approach) taking again into account the interdependencies of specific components. It is observed that the EQL approach is associated with higher number of non-functional components for all considered seismic scenarios whereas for the NL approach non-functional components are present only for the 4975 years scenario I. The estimated PIs of the port are normalized to the respective value referring to non-seismic conditions (Table 2). As also evidenced by the estimated functionality state of each component, the port system is non-functional both in terms of TCaH and TCoH for the 4975 years scenario I. A 100% and 67% performance loss is estimated for the TCoH and TCaH respectively when considering the EQL approach for the 475 and 4975 years II scenarios, while the port is fully functional when considering the NL approach both in terms of TCaH and TCoH for the latter scenarios. Further details regarding the scenario based risk assessment are provided in [4].

5. Decision Phase and Conclusions

An important aspect of the stress test framework is the comparison of the risk assessment results with the defined risk objectives to check whether the port system passes, partially passes or fails the stress test and to define the grading system parameters for the next evaluation of the stress test since the performance of the CI or performance objectives can change over time [1]. In Fig. 4 (left panel) performance boundaries are plotted together with the MAF curves of the assessed performance loss. With reference to both bulk cargo and container terminals (TCaH, TCoH curves) the port obtains grade B, meaning that the risk is possibly unjustifiable and the CI partly passes this evaluation. The basis for redefinition of risk objectives in the next evaluation of stress test is the characteristic point of risk, which is defined as the point associated with the greatest risk above the ALARP region (blue and red dots for TCaH and TCoH curves respectively). These points are the farthest from the A-B boundary (blue line). The proposed grading system foresees the reduction of the boundary between grades B and C (red line) in the next stress test, which is equal to the amount of risk beyond the ALARP region assessed, represented in this application by the corresponding red dashed lines in case of the bulk cargo and cargo terminals. The plot in Fig. 4 (middle panel) indicates that the CI receives grade AA (negligible risk), and as expected in this example application, passes the stress test for the tsunami hazard. Indicative scalar performance boundaries in terms of the normalized performance loss are shown in Table 2 together with the corresponding results of the scenario based assessment. It is seen that the CI may pass, partly pass or fail the specific evaluation of the stress test depending on the selected seismic scenario, the analysis approach and the considered risk metric (TCaH, TCoH). The final phase of the methodology includes identification of the critical components and events as well as risk mitigation strategies to upgrade the port operations and improve its resilience. It is noted that, the risk objectives and the time between successive stress tests should be defined by the CI authority and regulator. Since regulatory requirements do not yet exist for all the CIs, the boundaries need to rely on judgements.

6. Acknowledgements

The work reported in this paper was carried out in the framework of STREST project, funded by the European Community's Seventh Framework Programme (FP7/2007-2013) under grant agreement no. 603389. The

contribution of Volpe M, Tonini R, Romano F, Brizuela B, Piatanesi A, Basili R, Lorito S. (INGV, Italy) in the tsunami hazard analysis is also acknowledged.

7. Copyrights

8. References

[1] Esposito S, Stojadinović B, Babič A, Dolšek M, Iqbal S, Selva J (2017): Engineering risk-based methodology and grading system for stress testing of critical non-nuclear infrastructures (STREST Project), *16th World Conference on Earthquake Engineering*, 9-13 January 2017, Santiago, Chile.

[2] Pitilakis K, Crowley H., Kaynia A (Eds) (2014a): SYNER-G: Typology definition and fragility functions for physical elements at seismic risk. Buildings, lifelines, transportation networks and critical facilities. *Geotechnical, Geological and Earthquake Engineering*, **27**, Springer, Netherlands.

[3] Anastasiadis A, Raptakis D, Pitilakis K (2001): Thessaloniki's detailed microzoning: subsurface structure as basis for site response analysis, *Pure and Applied Geophysics,* **158**, 2597-2633.

[4] Pitilakis K. et al. (2016): Deliverable D6.1: Integrated report detailing analyses, results and proposed hierarchical set of stress tests for the six CIs covered in STREST, STREST project: Harmonized approach to stress tests for critical infrastructures against natural hazards.

[5] National Institute of Building Sciences, NIBS (2004): Direct physical damage—general building stock. *HAZUS-MH Technical manual*, Chapter 5. Federal Emergency Management Agency, Washington, D.C

[6] Karafagka S, Fotopoulou S, Pitilakis K (2016): Tsunami fragility curves for seaport structures, *1st International Conference on Natural Hazards & Infrastructure*, 28-30 June 2016, Chania, Greece.

[7] Kappos AJ, Panagopoulos G, Panagiotopoulos C, Penelis G (2006): A hybrid method for the vulnerability assessment of R/C and URM buildings. *Bulletin of Earthquake Engineering*, **4**, 391-419.

[8] UPGRADE (2015): Technical reports with the calculation results of the vulnerability of specific Greek port facilities (in Greek). Deliverable 8.2, Research project: Contemporary Evaluation Methodology of Seismic Vulnerability and Upgrade of Port Facilities, http://excellence.minedu.gov.gr/thales/en/thalesprojects/380174

[9] SRMLIFE (2007): Development of a global methodology for the vulnerability assessment and risk management of lifelines, infrastructures and critical facilities. Application to the metropolitan area of Thessaloniki. Research project, General Secretariat for Research and Technology, Greece (in greek).

[10] Fajfar P, Dolšek M (2012): A practice-oriented estimation of the failure probability of building structures. *Earthquake Engng Struct. Dyn*, **41** (3), 531–547.

[11] Lazar N, Dolšek M (2013): Application of the risk-based seismic design procedure to a reinforced concrete frame building, *4th ECCOMAS Thematic Conference on Computational Methods in Structural Dynamics and Earthquake Engineering*, M. Papadrakakis, V. Papadopoulos, V. Plevris (eds.) Kos Island, Greece, 12–14 June 2013.

[12] Silva V, Crowley H, Bazzuro P (2014): Risk-targeted hazard maps for Europe. *Second European Conference on Earthquake Engineering and Seismology*, Istanbul, 24-29 August, Turkey.

[13] Pitilakis K, Franchin P, Khazai B, Wenzel H. (Eds) (2014b): SYNER-G: Systemic seismic vulnerability and risk assessment of complex urban, utility, lifeline systems and critical facilities. Methodology and applications. *Geotechnical, Geological and Earthquake Engineering*, **31**, Springer, Netherlands.

[14] Kakderi et al. (2015): Deliverable 4.2: Guidelines for performance and consequences assessment of geographically distributed, non-nuclear critical infrastructures exposed to multiple natural hazards. STREST project EC/FP7 (2007-2013), grant agreement No: 603389.

[15] Cornell C, Krawinkler H (2000): Progress and challenges in seismic performance assessment. *PEER News 2000*, **3** (2).

[16] Selva, J (2013): Long-term multi-risk assessment: statistical treatment of interaction among risks. *Natural Hazards*, **67** (2), 701-722.

[17] Weatherill G, Esposito S, Iervolino I, Franchin P, Cavalieri F (2014): Framework for seismic hazard analysis of spatially distributed systems, in: K. Pitilakis et al. (eds). Systemic seismic vulnerability and risk assessment of complex urban, utility, lifeline systems and critical facilities. Methodology and applications. Springer, Netherlands, 57-88.

[18] Giardini D. et al. (2013): Seismic Hazard Harmonization in Europe (SHARE). Online Data Resource, http://portal.share-eu.org:8080/jetspeed/portal/, doi: 10.12686/SED-00000001-SHARE, 2013.

[19] Akkar S, Bommer JJ (2010): Empirical equations for the prediction of PGA, PGV and spectral accelerations in Europe, the Mediterranean and the Middle East. *Seismol Res Lett*, **81**, 195–206.

[20] Jayaram N, Baker JW (2009): Correlation model of spatially distributed ground motion intensities. *Earthquake Engineering and Structural Dynamics*, **38** (15), 1687–1708.

[21] EN 1998-1 (2004): Eurocode 8: Design of structures for earthquake resistance-Part 1: General rules, seismic actions and rules for buildings. CEN, Bruxelles, 2004.

[22] Lorito S, Selva J, Basili R, Romano F, Tiberti MM. Piatanesi A (2015): Probabilistic hazard for seismically-induced tsunamis: accuracy and feasibility of inundation maps, *Geophys. J. Int.*, **200** (1), 574-588.

[23] Volpe M, Selva J, Tonini R, Romano F, Brizuela B, Piatanesi A, Basili R, Lorito S, in prep: From regional to site specific SPTHA through inundation simulations: a case study for Milazzo (Italy) and Thessaloniki (Greece).

[24] Parsons T, Geist EL (2009): Tsunami probability in the Caribbean region, *Pure appl. Geophys*., **165**, 2089–2116.

[25] Selva J, Tonini R, Molinari I, Tiberti MM, Romano F, Grezio A, Melini D, Piatanesi A, Basili R, Lorito S (2016a): Quantification of source uncertainties in Seismic Probabilistic Tsunami Hazard Analysis (SPTHA), *Geophys. J. Int*., doi:10.1093/gji/ggw107.

[26] Selva J, Tonini R, Romano F, Volpe M, Brizuela B, Piatanesi A, Basili R, Lorito S (2016b): From regional to site specific SPTHA through inundation simulations: a case study for three test sites in Central Mediterranean, *EGU General Assembly 2016*, 17-22 April, Vienna, Austria, Abstract #EGU2016-16988.

[27] Basili R, Tiberti MM, Kastelic V, Piatanesi A, Selva J, Lorito S (2013): Integrating geologic fault data into tsunami hazard studies, *Natural Hazards and Earth System Sciences*, **13**, 1025-1050, DOI: 10.5194/nhess-13-1025-2013.

[28] Molinari I, Tonini R, Piatanesi A, Lorito S, Romano F, Melini D, Gonzalez Vida JM, Macias J, Castro M, de la Asuncion M (2016): Fast evaluation of tsunami scenarios: uncertainty assessment for a Mediterranean Sea database, submitted to NHESS (under review).

[29] Marzocchi W, Taroni M, Selva J (2015): Accounting for epistemic uncertainty in PSHA: logic tree and ensemble modeling, Bulletin of the Seismological Society of America, 105 (4), doi: 10.1785/0120140131.

[30] Gonzalez Vida JM et al, (2015): Tsunami-HySEA: a GPU based model for the Italian candidate tsunami service provider, *EGU General Assembly 2015*, 12-17 April, Vienna, Austria, Abstract # EGU2015-13797.

[31] Papaioannou C (2004): Seismic hazard scenarios-Probabilistic seismic hazard analysis, SRM-Life Project: Development of a global methodology for the vulnerability assessment and risk management of lifelines, infrastructures and critical facilities. Application to the metropolitan area of Thessaloniki (in greek).

[32] Smerzini C, Pitilakis K, Hasmemi K, submitted: Evaluation of earthquake ground motion and site effects in the Thessaloniki urban area by 3D finite-fault numerical simulations, Bulletin of Earthquake Engineering.

[33] Kottke AR, Rathje EM (2008): Technical Manual for Strata. *PEER Report 2008/10*. University of California, Berkeley.

[34] Elgamal A, Yang Z, Lu J (2015): Cyclic1D Seismic Ground Response Version 1.4, User's Manual, University of California, San Diego, Department of Structural Engineering.

[35] Toro GR (1995): Probablistic models of site velocity profiles for generic and site-specific ground-motion amplification studies. Upton, New York: Brookhaven National Laboratory.